# Scaling and synchronization methods from statistical physics applied to physiological data

**Ronny Bartsch**
Department of Physics

Ph. D. Thesis

Submitted to the Senate of Bar-Ilan University

Ramat-Gan, Israel April 15, 2008

This research was carried out under the supervision of

Prof. Shlomo Havlin

(Department of Physics)
Bar-Ilan University.

**Acknowledgments:** I wish to express my deepest gratitude to Professor Shlomo Havlin for his guidance and support of my Ph.D. studies.

I am also very grateful to my closest collaborator, Professor Jan Kantelhardt, for many fruitful discussions and his assistance during my research, as well as the excellent hospitality during my frequent visits to Halle. I thank my closest clinical collaborator, Dr. Meir Plotnik, for inspiring me with gait analysis, giving me better physiological understanding and supporting me in all circumstances. I thank Professor Jeff Hausdorff for many motivating discussions and ideas, and for welcoming me in his "gait-research-group" in Ichilov. I am also very grateful to Professor Thomas Penzel for providing an unique data set for our sleep project.

I deeply appreciate the financial support of the Minerva foundation in Germany, and the President's scholarship for excellent Ph.D. students ("Milgat Nasi") in Bar-Ilan University. Without these two scholarships, my Ph.D. studies would not have been possible.

Many thanks to my dear colleagues, Shay Moshel, Avi Gozolchiani, Nilly Madar, Amir Bashan, Avi Cohen, Shai Carmi, Roni Parshani, Diego Rybski, Lukas Jahnke, Aicko Schumann, Isabella Osetinsky, Valerie Livina, Dov Nagar, Igor Zhidkov, and Tomer Kalisky for their friendship, support and the nice time we spent together in Israel and at Bar-Ilan University. I also thank the gait-research-group in Ichilov for very friendly working conditions.

Thanks a lot to Diego and Jan for reading the manuscript of this thesis and providing feedback. Special thanks goes to Nilly for helping me with the Hebrew part of my thesis.

Last but not least I thank my family with all my heart, especially my parents and Iris, for their constant encouragement, permanent support and faithful belief in me, my work and my studies.

# Contents



1) A. Bashan, R. Bartsch, J.W. Kantelhardt, and S. Havlin. Comparison of detrending methods for fluctuation analysis. Accepted for publication in *Physica A*, 2008.

2) R. Bartsch, M. Plotnik, J.W. Kantelhardt, S. Havlin, N. Giladi, and J.M. Hausdorff. Fluctuation and synchronization of gait intervals and gait force profiles distinguish stages of Parkinson's disease. *Physica A*, 383:455-465, 2007.

3) R. Bartsch, J.W. Kantelhardt, T. Penzel, and S. Havlin. Experimental evidence for phase synchronization transitions in the human cardiorespiratory system. *Physical Review Letters*, 98:054102(4), 2007.

# List of Figures

# 1 Abstract

The main purpose of my Ph.D. studies was to analyze scaling properties in physiological data and to study interrelations between physiological signals of the autonomic nervous system during sleep, as well as between signals of the neuromotor system during gait.

A systematic study of sleep data derived from 112 healthy subjects suggests an alternating influence of the brain upon the interrelations between the cardio and the respiratory system. In particular we demonstrated that the weak coupling between heartbeat and breathing, measured by cardio-respiratory synchronization, is disturbed during rapid-eye-movement (REM) sleep when higher brain regions show increased activity. On the other hand, during non-REM sleep when the brain is less active, we could show that cardio-respiratory synchronization is significantly enhanced.

In order to gain insight into the mechanism of cardio-respiratory coupling, we investigated the distribution of different synchronization patterns and their variation across sleep stages and with age. A comparison of synchronization patterns detected in the real signals with synchronization patterns found in surrogate data revealed that only $n:1$ synchronization (i.e. $n$ heartbeats synchronize with one breathing cycle) is effective. This observation provides an elegant way to conclude that cardio-respiratory coupling is mainly based on an unilateral interaction of the respiratory oscillator upon the heartbeat oscillator and not vice versa.

In another study, the gait force profile data of patients in different stages of Parkinson's disease (PD) and healthy elderly subjects were investigated. We found that long-term correlations in gait timing are significantly reduced for patients with advanced PD and de novo PD (i.e. PD in an early stage where patients were not treated yet) compared to the healthy controls. Surprisingly, long-term correlations in time series characterizing morphological changes in the force profiles were relatively weak for treated PD patients and healthy controls, while they were significantly larger for de novo PD patients. One possible explanation for this behavior is that long-term usage of anti-parkinsonian medication attenuates fluctuations in the morphology of gait force profiles, but not fluctuations in gait cycle timing.

In summary, the results obtained in this research are important to better understand patho-

logical and physiological mechanisms influencing neuromotor control and the autonomic nervous system. The present research led to the discovery of a new physiological phenomenon, namely that cardio-respiratory coupling is significantly effected by different sleep stages. Furthermore, it is an important step on the way to a novel method which detects early changes from normal to parkinsonian gait.

# 2 Introduction

Statistical physics plays a central role in investigating and describing macroscopic systems. Obviously, due to the complexity of such systems and their very high degrees of freedom, it is impossible to study macroscopic systems by a set of differential equations focusing on the motion of each constituent. On the other hand, the macroscopic quantities, which we are interested in, do not depend on the motions of individual particles. Instead, these quantities are governed by the average motions of all particles in the system. One way to gain insight into statistical properties of complex macroscopic systems is to analyze sequences of time observations. These time series, which represent consecutive measurements taken at equally spaced time intervals, describe the evolution of the system over time and allow the description of many phenomena especially in the thermodynamics of phase transitions. Another application where time series analysis is used, is to investigate complex biological processes and systems. In recent years, physiological systems under regulation of the autonomous nervous system (e.g. the heart) and under control of the neuromotor system (e.g. the limbs during movement and locomotion) were recognized as good models of complex systems. This is since, (i) physiological systems often include multiple components, thus leading to very high degrees of freedom, and (ii) physiological systems are usually driven by competing forces, e.g. parasympathetic versus sympathetic stimuli, extensor versus flexor etc. Therefore, it seems reasonable that physiological systems under neural regulation may exhibit temporal structures which are similar, under certain conditions, to those found in physical systems. Indeed, new conceptual frameworks and corresponding methodologies that originated in statistical physics are showing promise as useful tools for quantitative analysis of complex physiological systems.

Traditionally, physiological systems are considered as operating according to the classical principle of homeostasis, which postulates that a system returns to equilibrium after perturbation and that linear causality controls the pathways of physiological interaction [18, 33, 82]. Such classical systems are often characterized by a *single* dominant time scale which is related to the time interval the system needs to reach equilibrium after perturbation. In the last decade, however, empirical observations have shown that even under healthy basal conditions, physiologic systems exhibit "noisy" fluctuations, i.e. point to point deviations from a local average, with self-similar (fractal) organization over *multiple time* scales [4, 34, 35, 38, 44], resembling the

scale-invariant patterns found in the fluctuations of physical systems away from equilibrium. Since fluctuations are traditionally ignored in physiological and clinical studies, which are usually based on averaged quantities, the question was raised whether, (a) physiologic fluctuations simply reflect the fact that physiological systems are being constantly perturbed by external and intrinsic noise, or (b) do they contain useful, "hidden" information about the underlying control mechanisms and the interaction between physiological systems.

So far, previous studies have supported hypothesis (b), showing that physiological dynamics can be considered as an integrative result of a system or network of nonlinear feedback interactions [12, 36, 55]. As observed in modeled data, such systems never settle down to constant output, but rather exhibit complex scale-invariant fluctuations [15, 49, 76] similar to those found in physiologic data. Furthermore, it has been demonstrated that these fluctuations are characterized by the absence of a typical dominant time scale, and that they exhibit *scale-free* power-law behavior over a broad range of scales [77].

The results of the present Ph.D.-project further support hypothesis (b) by showing that also the fluctuations arising from interrelations between physiological systems are carrying essential information about underlying physiological control mechanisms. A main topic of the project was the investigation of interrelations between the brain and other physiological systems. In particular, we could demonstrate that the coupling between heartbeat and breathing is very sensitive to the sleep stages, and hence to autonomous control mechanisms of the brain [6]. Our assumption that the increased activity of higher brain regions during rapid-eye-movement (REM) sleep influences directly other physiological systems was tested by constructing physiological networks of polysomnographic data in different sleep stages [11]. Brain activity was thereby measured by electroencephalography (EEG) and, indeed, preliminary results show a clear difference in the network links associated with a coupling between the brain and the cardio-respiratory system. While in non-REM sleep there is no link between the cardio-respiratory system and EEG, the connection becomes evident in REM sleep. This finding supports a conjecture made earlier after analyzing separately heartbeat [16] and breathing data [68] in different sleep stages. In these works, a different correlation behavior of heartbeat and breathing intervals in different sleep stages led to the conclusion that the coupling strength between the cardio-respiratory system and the brain changes across sleep stages.

# 3 Theoretical Background and Previous Studies

An often observed phenomenon in physiological time series is the fact that their elements are correlated with each other over many time scales. This behavior was found to be very useful, for instance in distinguishing heart failure from normal subjects. By applying *Detrended Fluctuation Analysis* (DFA), an advanced method from statistical physics to quantify correlations in nonstationary time series (see Section 5.1.3), it has been shown that under normal conditions, beat-to-beat time interval fluctuations in heartbeat time series exhibit *long-range power-law correlations* over time scales from seconds to many hours [37, 57, 58]. Such robust scaling indicates the presence of a self-similar (fractal) hierarchical organization in heartbeat fluctuations and can not be explained by the classical principle of homeostasis. In contrast, heartbeat time series from patients with congestive heart failure show a breakdown of this long-range correlation behavior [4, 5, 29, 34, 35, 57] suggesting a direct link between the observed scaling features and the underlying intrinsic mechanism of cardiac regulation. Determining the correlation behavior of heart rate time series by means of DFA is also useful to study physiologic transitions of cardiac dynamics from rest to intense exercise [43], from wake to sleep [37], or across different sleep stages [16]. While, for example, long-range correlations are present in heartbeat intervals measured during rapid eye movement (REM) sleep, the data are uncorrelated during non-REM sleep [16, 39]. In the past decade, the DFA-method was also intensively used to analyze correlation properties in human gait [26, 27], and it has been demonstrated that there are reduced stride-to-stride time interval correlations in elderly subjects and patients with Huntington's disease. In addition there is a suggestion that gait data derived during "freezing-of-gait", a phenomenon that is common among patients with advanced Parkinson's disease (PD), are not random and show a fairly organized pattern.

A different way to analyze time series is to look for (multi-) fractal properties of the signal. One can do this by applying the *Wavelet Transform Modulus Maxima* (WTMM) method (see Section 5.1.5). Using the WTMM method has shown that heartbeat interval time series from healthy individuals and heart failure patients clearly differ in their scaling exponents [3]. Further work revealed that interbeat interval time series from healthy subjects and heart failure patients have a completely different fractal behavior: while interbeat interval time series from healthy subjects show multifractal properties, the loss of multifractality is an indication

of congestive heart failure [35]. Multifractal analysis was also applied on data measuring human balance, gait and posture. Recent work, where wavelet-based multifractal methods were employed to center of pressure traces of healthy subjects and patients with PD, has shown that the multifractal spectra for PD patients are narrower as compared to the healthy group, suggesting a reduction in complexity of the underlying control mechanisms in the neuromotor system [50]. Studying the multifractal spectra of human posture data further disclosed that the dominant fractal exponent becomes smaller and the range of fractal exponents strongly narrows if balance control inputs, such as visual cues or tactile information are reduced [75].

In addition to correlation and fractal properties, characteristic frequencies in time series are very important. In nonstationary signals, however, where the component frequencies change over time, it is of particular interest when certain frequencies occur. The most popular method of detecting frequencies – the Fourier transform – fails to provide this information. This is because Fourier transform averages the key features of a time-varying signal over the entire length of the signal and thus fine details are lost. As explained in, for example [2, 13, 19], this information can be found by applying wavelet analysis (see Section 5.1.4).
In case of human heartbeat interval time series, the standard deviation of wavelet coefficients, $\sigma_{\mathrm{wav}}(s)$, is especially interesting and has been shown to provide an exact discrimination between normal and heart failure subjects [80]. Particularly noteworthy is the fact that this separation was found on wavelet scales $s = 2^4 - 2^5$ corresponding to a frequency interval of $0.04 - 0.09$ Hz. This interval is part of the Low-Frequency-Band (LF-Band) which shows balance and disturbance of the autonomic nervous system [1].

The above mentioned research and methods were focusing on single physiological signals. To study dependencies in the dynamics between two or more physiological signals, two different methods can be applied. One of these methods is built upon the study of the cross-correlations and essentially compares the amplitude records. Another method provides an alternative way and is based on the phase synchronization approach.
*Cross-correlation Analysis* is a widely used method to study interrelations between two time series and to estimate time delays in biological systems (see e.g. [52]). The method of *Phase Synchronization Analysis* (PSA) (see Section 5.2.3) was recently elaborated within the theory

of weakly coupled chaotic oscillators [61, 66]. A known effect in these multi-component systems is the entrainment of phases between their components. *Phase Synchronization Analysis* is especially useful when the mechanisms which connect the components' dynamics are not clear. Revealing phenomena such as synchronized phases, phase locking or fixed time delays between physiological signals can supply rich and useful information about the underlying dynamics. By using PSA, it has been demonstrated that, in contrast to the common view among experts [23], phase synchronization between heartbeat and respiration exists [72]. This phenomenon, which was first found in athletes [71, 72], suggests a weak coupling between the heartbeat and the breathing oscillator, and is already present in infants [51, 65] but also in patients after heart transplantation [81]. Another application of PSA led to the identification of a group of neurons oscillating in close synchronization with the observed tremor in Parkinson's disease [79], a discovery which may be used to develop a novel treatment for this condition.

# 4 Summary and Significance of the Present Research

In Section 3 was shown that most of the past research was done on data series derived from time events in single physiological signals (for example interbeat intervals in human electrocardiograms (ECGs) or stride-to-stride time intervals in human gait). The present Ph.D.-project evaluated the importance of morphological information, especially the shape of force profiles in human gait. The other main objective of this study was the investigation of interrelations between physiological signals. A matter of particular interest was here the influence of the brain upon the coupling between heartbeat and respiration in different sleep stages of healthy subjects.

In the first part of my Ph.D. studies, several recently suggested methods for the detection of long-range correlations were examined to provide a theoretical basis for further research on physiological data. As it is well-known, techniques based on random walk theory are superior to the traditionally used (auto-) correlation function when quantifying correlations and memory in time series. However, the intrinsic correlations and fluctuations we are interested in, have to be well distinguished from non-stationarities (i.e. varying mean and standard deviation) and trends, which often appear in experimental data. Therefore, detrending of data is a very important step in time series analysis and several approaches have been introduced to cope with this task.

In our work [10], we evaluate different detrending techniques based, for instance, on empirical mode decomposition, singular value decomposition or different digital high-pass filters. Moreover, we present a detailed comparison between the well-established *Detrended Fluctuation Analysis* (DFA) and two other prominent detrending methods: the *Centered Moving Average* (CMA) Method and a *Modified Detrended Fluctuation Analysis* (MDFA). We find that CMA is performing equivalently as DFA in long data with weak trends but is superior to DFA in short data with weak trends. This important finding was used in later studies of human gait (see below). When comparing standard DFA to MDFA we observe that DFA performs slightly better in almost all examples we studied. We also discuss how several types of trends affect these methods. For example, in case of weak trends in the data, the new methods are comparable with DFA. However, if the functional form of the trend is not a-priori known, DFA remains the method of choice. Only a comparison of DFA results, using different detrending polynomials,

yields full recognition of the trends. A comparison with independent methods is recommended for proving long-range correlations.

As this work was assisting us choosing the appropriate methods and avoiding pitfalls during analyzes of physiological records, we believe that our article is a good review and guideline to other researchers who study long-range correlations in physiological data.

Based on the theoretical studies presented in [10], DFA, CMA and a corrected version of DFA were applied to gait data from 29 patients with advanced Parkinson's disease (PD), 13 subjects with de novo PD (i.e. PD patients, who were not treated yet with medication) and 24 healthy elderly subjects [8].

To study the data of each subject and each leg, we generated two different time series. First we used the series of time differences between two consecutive heel-strikes of one leg to define stride-to-stride time intervals. These series do not contain any information about the shape of the force profiles during stance time. Therefore, we extracted a second time series from the morphology of the gait force profiles in order to study their fluctuations over time.

We find that long-term correlations in gait timing (as expressed by the series of interstride intervals) are significantly reduced for PD patients and de novo PD patients compared to age-matched healthy controls. Surprisingly, long-term correlations of the series characterizing morphological changes in gait force profiles are relatively weak for treated PD patients and healthy controls, while they are significantly larger for de novo PD patients. We argue that this may be due to the long-term usage of anti-parkinsonian medication which attenuates fluctuations in the morphology of gait force profiles, but not fluctuations in gait cycle timing. The presented study also confirms that long-term gait variability in the timing of consecutive gait cycles is a marker for Parkinsonian gait. Another important outcome of our research is that timing and morphology of recordings obtained from a complex system can contain complementary information (see also [5] for a similar study on ECG recordings).

In order to quantify bilateral coordination between both legs during walking, we developed a new phase synchronization algorithm for human gait [8] (see also Section 5.2.2). When studying phase synchronization between right and left leg during walking, we demonstrate that both types of PD patients walk less synchronized compared to the group of healthy elderly subjects. We also show that performing different walking tasks (e.g. turns, slow walking) reduces

bilateral coordination between the right and the left leg [9]. These findings are of particular importance to gain insight into gait synchronization and its relation to the "freezing-of-gait" phenomenon, a very delimiting phenomenon common among patients with advanced Parkinson's disease which occurs especially after turns or changes in walking direction or velocity.

The main part of my Ph.D. studies was, however, the analysis of interrelations between physiological signals. By studying phase synchronization in polysomnographic data of healthy subjects we found *Experimental evidence for phase synchronization transitions in the human cardio-respiratory system* [6].

Firstly we developed an automated phase synchronization detector, which quantifies the degree and type of synchronization of two physiological signals. The technique is based on the automated study of cardio-respiratory synchrograms (see Section 5.2.3). We employed this procedure for screening the synchrograms of 112 healthy subjects studying the frequency and the distribution of synchronization episodes under different well-defined physiological conditions that occur during sleep.

We find that phase synchronization between heartbeat and breathing is significantly reduced during rapid-eye-movement (REM) sleep and enhanced during non-REM sleep (deep sleep and light sleep). This result is independent of age, gender and physical condition, suggesting a fundamental physiological mechanism. Our results further suggest that there is an alternating influence of the brain upon the weak coupling between the heartbeat and the breathing oscillator, a phenomenon which was up to now only observed in animal experiments [46, 59, 60]. During REM sleep, when the activity of higher brain regions is largely increased, cardio-respiratory coupling is perturbed and the phase of both rhythms can not be entrained. On the other hand, during non-REM sleep when the brain is less active, phase synchronization can be effective.

In the next step we directly study the distribution of different synchronization ratios, $n:m$ where $n$ is the number of heartbeats synchronized with $m$ breathing cycles (see Section 5.2.3). Based on the quotient of the synchronization ratio histogram with the distribution of frequency ratios between heartbeat and breathing (independent of synchronization) we prove that $n:1$ synchronization is more effective than synchronization ratios of order $n:2$ and $n:3$. Moreover, a detailed comparison with surrogate data constructed by random combination of heartbeat and breathing signals from different subjects, reveals that the occurrence of $n:2$ and $n:3$ may

be more accidental. This observation can be explained by an asymmetry in cardio-respiratory coupling when the breathing oscillator is driving the heartbeat oscillator and not vice versa (see also [65] for a more mathematical approach to determine this directionality).

The influence of the brain upon other physiological systems was studied directly by a newly developed cross correlation method in which links for interrelated signals of very different origin can be established (see Section 5.2.4). In this manner, so-called *physiological networks* are constructed from polysomnographic data collected during different sleep stages. Preliminary results of this approach show that for example in deep sleep (DS), the brain is less "connected" to other physiological systems (e.g. to the cardio-respiratory system, to the muscular system, to blood pressure, and to eye movements). On the other hand, during REM sleep we find high connectivity [11]. This finding supports our and former assumptions that the brain influences the heartbeat [16] and the breathing oscillator [68] as well as cardio-respiratory coupling [6] during REM but not during non-REM sleep.

Another interesting finding is that specific synchronization patterns in cardio-respiratory synchronization and, in particular, the efficiency of cardio-respiratory synchronization changes with age [7]. However, the medical relevance of cardio-respiratory synchronization is not well understood yet. This might be due to the absence of long-term breathing recordings of subjects performing regular daily activities. In another project we therefore study the ability of several methods in reconstructing breathing data from long-term ECGs. The outcome of this work is used to analyze cardio-respiratory synchronization based on 24 hours ECGs from more than 1000 patients after myocardial infarction. Preliminary results suggest that an increased level of synchronization might have an adverse effect in surviving a period of five years after the cardiac incident [25].

In summary, the main contributions of this Ph.D.-project are:

1. The definition of time series characterizing morphological changes of gait force profiles whose different fluctuation patterns provide discrimination between patients with Parkinson's disease in different stages, and hence may be useful to detect early changes from physiology to pathophysiology and study effects of treatment.

2. The development of a synchronization algorithm which quantifies bilateral coordination during walking. Using this algorithm we show for the first time that (i) parkinsonian gait

is less synchronized than normal gait, and (ii) the freezing-of-gait phenomenon seems to be due to lack of synchronization.

3. The development of a method which automatically detects cardio-respiratory synchronization and quantifies cardio-respiratory synchrograms. With this method we were able to discover a new physiological phenomenon, namely that cardio-respiratory coupling is significantly effected by different sleep stages. This finding is an important contribution to the ongoing discussion about alternating influences of the brain on other physiological systems during sleep, which was so far only observed in animal experiments.

4. The definition of cardio-respiratory efficiency which provides an elegant and simple way to argue about coupling directions in the cardio-respiratory system.

5. The development of a new cross correlation algorithm which enables the study of interrelations between physiological signals of very different origin. Based on this algorithm, physiological networks have been constructed which confirm the assumption of an alternating influence of the brain upon physiological systems during sleep. We strongly believe that this physiological network approach will open a new field of physiological data analysis.

# 5 Methodology

In this section I present the statistical physics concepts and methods which were used during my research. The first part describes methods for the quantification of long-term (auto) correlations and multifractality. The subject of the second part are interrelations between signals which we studied by newly developed methods of phase synchronization and cross-correlation analysis. If not otherwise stated, we consider in the following paragraphs time series $\mathcal{X}$ and $\mathcal{Z}$, consisting of values $x_i$ and $z_i$ $(i = 1, \ldots, N)$ measured in equidistant time intervals.

## 5.1 Quantifying Long-Term Correlations and Multifractality

The standard approach to quantify correlations within a time series $\mathcal{X}$ is calculating the auto-covariance or the autocorrelation function

$$C^{\mathrm{V}}(s) = \frac{1}{(N-s)} \sum_{i=1}^{N-s} (x_i - \langle x \rangle)(x_{i+s} - \langle x \rangle) \qquad \text{(autocovariance function)} \tag{1}$$

$$C(s) = C^{\mathrm{V}}(s)/C^{\mathrm{V}}(0) \qquad \text{(autocorrelation function)}, \tag{2}$$

where $\langle x \rangle$ is the mean of $\mathcal{X}$, and $s$ is the time lag between two elements in $\mathcal{X}$.
In case that $C(s)$ decays slowly for large $s$, such as

$$C(s) \sim s^{-\gamma} \qquad \text{with } 0 < \gamma < 1, \tag{3}$$

the characteristic correlation time,

$$s_\times = \int_0^\infty C(s) \mathrm{d}s, \tag{4}$$

diverges and therefore this correlation behavior is called to be of long term. On the other hand, if the integral in Eq. (4) converges, e.g. for $C(s) \sim \exp(-s/s_\times)$ or $C(s) \sim s^{-\gamma}$ with $\gamma > 1$, and $s_\times > 0$, the data in $\mathcal{X}$ are short-term correlated.

Quite often, however, $C(s)$ is hard to determine, in particular in the case of long-term correlations: for large time lags $s$, $C(s)$ greatly fluctuates around zero and an accurate scaling behavior can not be found. Furthermore a direct calculation of $C(s)$ can lead to a spurious detection of long-term correlations in uncorrelated data with trends [17]. Instead of calculating the autocorrelation function directly, several other methods were suggested that determine the correlation exponent $\gamma$ indirectly.

### 5.1.1 Hurst's Rescaled Range (R/S) Analysis

One of the first methods for quantifying long-term correlations was developed by Hurst [21, 30–32] when studying of how high the Aswan dam in Egypt had to be build in order to handle the greatly varying levels of the Nile within a given time window of observation, $s$. Taken retrospective records of water levels, $\mathcal{X}$, Hurst assumed a uniform outflow of the dam given by the mean of the varying inflow, $\langle x\rangle^{(s)} = (1/s)\sum_{i=1}^{s} x_i$. The change of water volume in the dam within the time window $s$ is given by the summed difference of inflow and outflow, $Y^{(s)}(m) = \sum_{i=1}^{m}(x_i - \langle x\rangle^{(s)})$. Hence, the range $R(s) = Y^{(s)}_{\max}(m) - Y^{(s)}_{\min}(m)$ of $Y^{(s)}(m)$ in $s$ determines how high the dam should be built that it neither overflows nor dries out. The ratio $R/S$ where $S$ is the standard deviation in $s$, $S(s) := \sigma^{(s)} = \sqrt{(1/s)\sum_{i=1}^{s}(x_i - \langle x\rangle^{(s)})^2}$, is a dimensionless quantity that showed, much to surprise of contemporary statisticians, a power-law scaling relationship with the length of observation, $s$:

$$(R/S)_s \sim s^H. \tag{5}$$

Later, Mandelbrot named this scaling exponent after Hurst and gave it the letter $H$. The relation between the Hurst exponent $H$ and the correlation exponent $\gamma$ is given by

$$H \simeq 1 - \frac{\gamma}{2} \tag{6}$$

(see Section 5.1.3).

### 5.1.2 Power Spectrum Analysis

While Hurst's R/S analysis studies data and its long-term correlations in the time domain, this section focuses on the description of long-term correlations in the frequency domain.

The transformation between time and frequency domain of a function $g(t)$ is done by the Fourier transform and the inverse Fourier transform, respectively [63]:

$$G(f) = \int_{-\infty}^{+\infty} g(t)\exp(-2\pi\imath f t)\mathrm{d}t \qquad \text{(Fourier transform)} \tag{7}$$

$$g(t) = \int_{-\infty}^{+\infty} G(f)\exp(2\pi\imath f t)\mathrm{d}f \qquad \text{(inverse Fourier transform).} \tag{8}$$

The complex function $G(f)$ defines the frequency spectrum

$$G(f) = |G(f)|\exp(\imath\varphi(f)) \tag{9}$$

with

$$|G(f)| = \sqrt{\Re(G(f))^2 + \Im(G(f))^2} \qquad \text{amplitude spectrum and} \tag{10}$$

$$\varphi(f) = \arctan \frac{\Im(G(f))}{\Re(G(f))} \qquad \text{phase spectrum.} \tag{11}$$

In the following we will focus on two important applications of the Fourier transform, namely the power-spectral density, or power spectrum, of $g(t)$,

$$P_g(f) := |G(f)|^2, \text{ and} \tag{12}$$

the convolution theorem

$$h(t) * g(t) \longleftrightarrow H(f)G(f). \tag{13}$$

One calculates the convolution of two functions $h(t)$ and $g(t)$ according to

$$(h * g)(s) := \int_{-\infty}^{+\infty} h(\theta)g(s-\theta)\mathrm{d}\theta, \tag{14}$$

where $s$ is a time shift.

To study cross-correlations between $h(t)$ and $g(t)$ one defines the cross-covariance function

$$C_{\times}^{\mathrm{V};h,g}(s) := \lim_{k\to+\infty} \frac{1}{2k} \int_{-k}^{k} h(\theta)g(s+\theta)\mathrm{d}\theta, \tag{15}$$

which, by help of Eqs. (13) and (14), can be written as

$$C_{\times}^{\mathrm{V};h,g}(s) \longleftrightarrow H(-f)G(f) \tag{16}$$

($h(t)$ and $g(t)$ are assumed to be real functions).

In case of autocorrelations, when $h(t) \equiv g(t)$ one finds the Wiener-Khinchin-theorem [24],

$$C^{\mathrm{V};h}(s) \longleftrightarrow |H(f)|^2, \tag{17}$$

and with Eq. (12)

$$C^{\mathrm{V};h}(s) \longleftrightarrow P_h(f). \tag{18}$$

Assuming stationarity, i.e. all moments of $h(t)$ are constant over time, the power spectrum is given by the Fourier transform of the autocovariance (or autocorrelation) function.

In case of long-term correlations, when $C(s) \sim s^{-\gamma}$, it follows directly from Eq. (18) [14] that the power spectrum decays as

$$P_h(f) \sim f^{\gamma-1}. \tag{19}$$

Defining $\beta$ as scaling exponent of the power spectrum, i.e. $P(f) \sim f^{\beta}$, one finds from Eq. (19) [28] that

$$\beta = 1 - \gamma. \tag{20}$$

Equation (20) relates the spectral exponent $\beta$ with the correlation exponent $\gamma$ and leads to two important applications:

(i) Since the *Fast Fourier Transform* (FFT) provides a fast way to calculate the power spectrum, correlations can be determined in this way rather than computing the auto-correlation function directly.

(ii) With help of Eq. (19), one can generate long-term correlated random noise by multiplying the frequency spectrum of a Gaussian distributed uncorrelated time series with $f^{-\beta/2}$. The resulting power spectrum will thus decay with $\beta$ and after an inverse Fourier transform long-term correlated data are available. This procedure, called *Fourier Filter Method* (FFM), was further improved by Makse et al. [47] to avoid the singularity of $C(s)$ at $s = 0$. Furthermore it is also possible to generate long-term correlated data which do not have a Gaussian distribution [20, 73, 74].

### 5.1.3 Detrended Fluctuation Analysis (DFA)

A drawback of the above-mentioned methods is the spurious detection of correlations in data with trends [40, 56]. Here, trends are understood as systematic, not random, changes of the series' mean. A method which is able to quantify correlations in such data, especially when the underlying trends have a polynomial form, is *Detrended Fluctuation Analysis* (DFA) [56].

According to this method, one first derives the "profile" $X(n) = \sum_{i=1}^{n}(x_i - \langle x \rangle)$ of the series $\mathcal{X}$, which can be considered as the position of a random walker on a linear chain after $n$ steps. The profile is then divided into $N_s \equiv \mathrm{int}(N/s)$ non-overlapping segments of equal length $s$ and a polynomial trend $y_{\nu}^{(p)}(i)$ of order $p$ is subtracted from the profile in each segment $\nu$ ("detrending"). The variance $F^2(\nu, s)$ on scale $s$ in segment $\nu$ is now given by

$$F^2(\nu, s) = \frac{1}{s} \sum_{i=(\nu-1)s}^{\nu s} [\tilde{X}(i)]^2, \tag{21}$$

where

$$\tilde{X}(i) = X(i) - y_{\nu}^{(p)}(i) \tag{22}$$

is the detrended profile function. The order of the polynomial can be varied to eliminate linear ($p = 1$), quadratic ($p = 2$) or higher order trends of the profile function. Conventionally, the DFA is named after the order of the fitting polynomial (DFA1, DFA2, ...) [16, 17, 40]. An average over all $2N_s$ segments[1] of size $s$ yields the fluctuation function

$$F(s) = \left\{ \frac{1}{2N_s} \sum_{\nu=1}^{2N_s} [F^2(\nu, s)] \right\}^{\frac{1}{2}} . \tag{23}$$

The fluctuation function corresponds to the trend-eliminated root-mean-square displacement of the random walker mentioned above and is related to the autocorrelation function by an integral expression [40, 56, 78]. Hence, from the scaling behavior of $F^2(s)$ for increasing $s$ one can draw conclusions about $C(s)$ and therefore about the type of correlations in $\mathcal{X}$:

- In case of short-term correlations for which the data become uncorrelated above the correlation time $s_\times$ (see above),

  $$F^2(s) \sim s \qquad (\text{for } s > s_\times). \tag{24}$$

  This behavior of the mean-square fluctuations corresponds to the linear time law observed in regular diffusion, i.e. Fick's law.

- If long-term correlations are present in $\mathcal{X}$ (Eq. (3)), then

  $$F^2(s) \sim s^{2\alpha} \qquad \text{with } \alpha = 1 - \frac{\gamma}{2} \quad (0 < \gamma < 1) \text{ [21, 40, 56, 78]}, \tag{25}$$

  which corresponds to superdiffusion, if $\alpha > 0.5$, or subdiffusion, if $\alpha < 0.5$.

Summarizing, a value of $\alpha = 0.5$ indicates that there are no (or only short-term) correlations in the data. If $\alpha > 0.5$ the data in the series are long-term correlated and the higher $\alpha$ is, the stronger are the correlations in the signal. The case $\alpha < 0.5$ corresponds to long-term anticorrelations, meaning that large values are most likely to be followed by small values (see e.g. [5] for a detailed discussion). Note that DFA1 is comparable with Hurst's R/S-Analysis since both eliminate constant trends, namely means, in the original data series $\mathcal{X}$, and hence it is expected that $H \approx \alpha$ for monofractal records [41, 69] (see also Section 5.1.5).

There are several other modifications and extensions of DFA which mostly focus on the elimination of different kinds of trends in data. For an overview and discussion see [10].

[1] In order not to disregard parts of the series at the end, it was suggested [40] to calculate $F^2(\nu, s)$ also by starting from the other end of the record.

### 5.1.4 Wavelet Analysis

Wavelet analysis is usually used to detect periodicities in nonstationary signals [2, 13]. Furthermore it is the basis for the *Wavelet Transform Modulus Maxima* method to quantify multifractal properties in time series (see Section 5.1.5) and it provides a way to define the instantaneous phase of a signal (see Section 5.2.2).

The method of wavelet analysis is based on the continuous wavelet transform,

$$\mathcal{W}(g(t)) = \omega(a) \int_{-\infty}^{+\infty} g(t)\psi^* \left(\frac{t-b}{a}\right) \mathrm{d}t, \tag{26}$$

which is the convolution of a function $g(t)$ with a (complex) wavelet function $\psi^*(t)$ [13, 19]. The analyzing wavelet $\psi^*$ has a width of order $a$ ("frequency (or scale) parameter") and is centered around $b$ ("translation parameter"). The weighting function $\omega(a)$ is usually chosen as $\omega(a) = a^{-1/2}$. The difference between the wavelet transform and the Fourier transform is that $g(t)$ is convolved with a wavelet function instead of $\exp(-2\pi\imath ft)$, and since the wavelet can be adapted in scale and shifted in time, the wavelet transform provides additional information about local properties of $g(t)$.

In case of a time series, which is always a discrete signal $\mathcal{X}$, we discretize Eq. (26) and determine wavelet coefficients by [2]

$$W(j,k) = 2^{-j/2} \sum_{i=1}^{N} x_i \psi(2^{-j}i - k) \tag{27}$$

where $N$ is the length of the time series and $\psi$ is real[2]. The wavelets $\psi$ are typically chosen to be orthogonal to polynomials of order $p$ to remove trends within the data and hence, the wavelet coefficients are comparable with the detrended profile function in Eq. (22). In analogy to DFA, long-term correlations can therefore be found by studying the variance of the wavelet coefficients versus scale $s$. Taking the wavelet coefficient variance

$$\sigma^2_{\mathrm{wav}}(j) = \frac{1}{N_s - 1} \sum_{k=0}^{N_s-1} (W(j,k) - \langle W(j,k)\rangle)^2 \tag{28}$$

($N_s \equiv \mathrm{int}(N/s)$ with $s = 2^j$) and assuming that the wavelet coefficient mean vanishes, i.e.

[2]The discretization in a logarithmic scale to basis 2, i.e. $a = 2^j$ and $b = 2^j k$, is often used in practice since it allows calculation of the wavelet transform by numerically very efficient algorithms. However, for the WTMM method (see below), a linear scale is commonly used.

$\langle W(j,k)\rangle = 0$, it follows from Eq. (28) that

$$\sigma^2_{\mathrm{wav}}(s) \sim s \sum_k |W(s,k)|^2. \tag{29}$$

The wavelet coefficient variance often scales with $s$ by

$$\sigma^2_{\mathrm{wav}}(s) \sim s^{\delta+1}, \tag{30}$$

and because of the similarity between $F^2(s)$ (Section 5.1.3) and $\sigma^2_{\mathrm{wav}}(s)$ we expect

$$\delta \simeq 2\alpha - 1 \tag{31}$$

(see also Section 5.1.5).

### 5.1.5 Multifractal Analysis

Quite often the correlation behavior of real world time series is rather complex and can not be characterized by a single scaling exponent $\alpha$ or $\delta$. Instead, different scaling exponents are found for large or small fluctuations in different time windows ("multi-scaling") and therefore, in analogy to fractal mathematics, such signals are termed multifractals. The following two novel methods were used to study multifractal properties of time series.

**a) Multifractal Detrended Fluctuation Analysis (MF-DFA)**

The MF-DFA is a generalization of the DFA method introduced above [42]. Instead of taking the square root in Eq. (23), for MF-DFA we calculate the $q$th order fluctuation function,

$$F_q(s) = \left\{ \frac{1}{2N_s} \sum_{\nu=1}^{2N_s} [F^2(\nu,s)]^{q/2} \right\}^{\frac{1}{q}}, \tag{32}$$

which increases, for large values of $s$, as a power law,

$$F_q(s) \sim s^{\alpha(q)}. \tag{33}$$

The scaling exponent $\alpha(q)$ is called the generalized fluctuation exponent. Note that $\alpha(q=1)$ is equivalent to the Hurst exponent found by means of Hurst's R/S analysis (Section 5.1.1) and that MF-DFA is identical to standard DFA (Section 5.1.3) in case of $q = 2$. The generalized fluctuation exponent, $\alpha(q)$, describes the scaling behavior of $F_q(s)$ for segments with small fluctuations, if $q < 0$, and for segments with large fluctuations, if $q > 0$. If a time series is monofractal, in which the scaling behavior of the variances $F^2(\nu,s)$ is identical for all segments $\nu$, $\alpha(q)$ will be independent of $q$.

**b) Wavelet Transform Modulus Maxima (WTMM)**

The WTMM method is based on the continuous wavelet transform (see Eq. (26)) and wavelet coefficients are calculated by

$$W(a,b) = a^{-\frac{1}{2}} \sum_{i=1}^{N} x_i \psi \left( \frac{i-b}{a} \right). \tag{34}$$

According to the modulus maxima procedure [48], we sum up the $q$th power of all local maxima of $W(a,b)$ on scale $a$ and determine the partition function

$$Z(q,a) = \sum_{b=1}^{N/a} |W_{\max}(a,b)|^q. \tag{35}$$

In order to keep the dependence of $Z(q,a)$ on $a$ monotonous, an additional supremum operation has to be applied [53] and often a scaling behavior is observed for $Z(q,a)$ with $a$,

$$Z(q,a) \sim a^{\tau(q)}. \tag{36}$$

Note that for $q = 2$, the exponent $\tau$ is similar to the exponent $\delta$, introduced in Section 5.1.4.

The scaling exponents $\tau(q)$ characterize the multifractal properties of the series. If $\tau(q)$ versus $q$ shows a linear behavior, the time series is monofractal, if $\tau(q)$ is bent, the signal is a multifractal. The strength of multifractality is commonly measured by the width of the multifractal spectrum which can be calculated by a Legendre transform of $\tau(q)$ (see e.g. [53]).

The relation between $\tau(q)$ and the generalized fluctuation exponent, $\alpha(q)$, calculated by MF-DFA was derived in [42] and is given by

$$\tau(q) = q\alpha(q) - 1. \tag{37}$$

## 5.2 Quantifying Interrelations Between Two Signals

Section 5.1 introduced methods and algorithms which were developed to investigate scaling and multi-scaling properties of single physiological signals. In order to measure the interdependence between physiological signals other methods have to be applied. Two of the most common of such measures are based on phase synchronization and cross-correlation analysis. While phase

synchronization analysis was developed to study nonlinear interrelations between (quasi-) periodic signals, cross-correlation analysis is a linear measure and should be applied to investigate correlations in the signals' noise. However, a theoretical framework necessary to understand the relation between both methods and to state about their particular benefits/drawbacks requires a systematic research on different types of coupling which is still missing (see [64, 67, 70] for further discussions and comparative studies of both methods on real data).
In the following we give the common definitions for phase synchronization and cross-correlation and present established and newly developed methods for phase synchronization analysis and cross-correlation analysis.

### 5.2.1 Definition of Phase Synchronization

The phase dynamics of two weakly coupled oscillators with natural frequencies $\omega_1$ and $\omega_2$ can be written as

$$\frac{\mathrm{d}\phi_1}{\mathrm{d}t} = \omega_1 + \varepsilon g_1(\phi_1, \phi_2) \qquad \text{oscillator 1 and} \tag{38}$$

$$\frac{\mathrm{d}\phi_2}{\mathrm{d}t} = \omega_2 + \varepsilon g_2(\phi_2, \phi_1) \qquad \text{oscillator 2,} \tag{39}$$

where $g_{1,2}$ are $2\pi$ periodic coupling terms, and $\varepsilon$ is the coupling strength. In general, both oscillators are synchronized, if the difference of their phases is constant, i.e. [67]

$$|n\phi_1 - m\phi_2| = \text{const} \qquad \text{“phase locking”.} \tag{40}$$

The integer prefactors $n$ and $m$ are chosen according to the ratio of the natural frequencies of oscillator 1 and 2,

$$\frac{\omega_2}{\omega_1} = \frac{n}{m}. \tag{41}$$

In case of periodic oscillators, Eq. (40) is equivalent to

$$n\dot{\phi}_1 = m\dot{\phi}_2 \qquad \text{“frequency locking”.} \tag{42}$$

However, since real oscillators are affected by irregularities and noise, for practical purposes, Eq. (42) only holds approximately,

$$n\dot{\phi}_1 \approx m\dot{\phi}_2, \tag{43}$$

and can be written as

$$n\Omega_1 = m\Omega_2, \tag{44}$$

where $\Omega_{1,2} = \langle \frac{\mathrm{d}}{\mathrm{d}t}\phi_{1,2} \rangle$ are the mean frequencies of the coupled oscillators [71]. Because of the time averaging, Eq. (44) can be fulfilled even when the oscillators are not coupled (especially for identical oscillators with (nonidentical) weak noise). Therefore, synchronization has to be understood as phase locking. By integrating Eq. (43) one finds

$$|n\phi_1 - m\phi_2 - \Delta| < \text{const}, \tag{45}$$

where $\Delta$ is some constant of integration symbolizing a phase shift around which the generalized phase difference

$$\varphi_{n,m} = n\phi_1 - m\phi_2 \tag{46}$$

is fluctuating. In case of noise, phase slips are often observed leading to an unbounded phase difference (and violating condition (45)). Nevertheless, if phase locking in a statistical sense is present in the data, a dominant peak in the distribution of the cyclic relative phase [67],

$$\Psi_{n,m}(t) = \varphi_{n,m}(t) \bmod 2\pi, \tag{47}$$

will be found. This definition of phase locking is particularly important when studying real-world data, and we will discuss its application in Section 5.2.3.

### 5.2.2 Calculating the Phase of a Signal

The phase of a stable periodic oscillation can be defined by

$$\phi(\theta) = \omega_0 \int_0^{\theta} [\nu(\theta')]^{-1} \mathrm{d}\theta', \tag{48}$$

where $\nu(\theta) = \mathrm{d}\theta/\mathrm{d}t$ is the angular velocity, and the angular frequency $\omega_0 = 2\pi/T_0$ ($T_0$ is the period of the oscillation) is given by $2\pi = \omega_0 \int_0^{2\pi} [\nu(\theta')]^{-1} \mathrm{d}\theta'$. By means of equation (48) the phase can be calculated for all periodic oscillations with corresponding $\nu(\theta)$.

In practice, data are usually not strictly periodic and since $\nu(\theta)$ is not known for every time increment, other ways have to be found to estimate the instantaneous phase of a signal. If the signal can be seen as output of a simple point process, as for instance in heartbeat data, the phase is usually defined as a piece-wise linear function of time. Between two consecutive events (e.g. heartbeats), the phase increases linearly by $2\pi$ and can be determined according to [67]

$$\Phi(t) = 2\pi \frac{t - t_n}{t_{n+1} - t_n} + 2\pi n, \tag{49}$$

where $t_n \leq t \leq t_{n+1}$ and $t_n$ is the time of the n-th event.
In order to study synchronization in gait data and to take into account both, information about the timing of heel-strikes [hs] and toe-offs [to] in either leg, we developed an algorithm which directly calculates the phase difference between right and left leg:

$$\Delta\Phi_k^m = 2\pi \frac{t_k^{m,\mathrm{ri}} - t_k^{\mathrm{hs,le}}}{t_{k+1}^{\mathrm{hs,le}} - t_k^{\mathrm{hs,le}}}, \tag{50}$$

where $t_k^{m,\mathrm{ri}}$ refers either to the heel-strike (mode $m = \mathrm{hs}$) or the toe-off point ($m = \mathrm{to}$) of the right leg.
The resulting phase differences typically form a time series $\psi = (\Delta\Phi_1^{\mathrm{hs}}, \Delta\Phi_1^{\mathrm{to}}, \ldots, \Delta\Phi_k^{\mathrm{hs}}, \Delta\phi_k^{\mathrm{to}}, \ldots)$ with averages, $\langle\Delta\Phi^{\mathrm{hs}}\rangle \neq \langle\Delta\Phi^{\mathrm{to}}\rangle$. For the sake of a uniform analysis of $\Delta\Phi^{\mathrm{hs}}$ and $\Delta\Phi^{\mathrm{to}}$, we calculated the time series of the normalized phase differences $\tilde{\psi} = (\Delta\tilde{\Phi}_1^{\mathrm{hs}}, \Delta\tilde{\Phi}_1^{\mathrm{to}}, \ldots, \Delta\tilde{\Phi}_k^{\mathrm{hs}}, \Delta\tilde{\Phi}_k^{\mathrm{to}}, \ldots)$ with $\Delta\tilde{\Phi}_k^{\mathrm{hs}} = \Delta\Phi_k^{\mathrm{hs}} - 1/2(\langle\Delta\Phi^{\mathrm{hs}}\rangle - \langle\Delta\Phi^{\mathrm{to}}\rangle)$ and $\Delta\tilde{\Phi}_k^{\mathrm{to}} = \Delta\Phi_k^{\mathrm{to}} + 1/2(\langle\Delta\Phi^{\mathrm{hs}}\rangle - \langle\Delta\Phi^{\mathrm{to}}\rangle)$. The time series of normalized phase differences can now be directly evaluated by phase synchronization analysis (see Section 5.2.3).

Most physiological signals are very noisy or even chaotic. One approach for such signals is to extract the phase by the analytic signal concept introduced by Gabor [22]. This general method transforms a signal $g(t)$ into a complex process $\zeta(t)$ with an instantaneous amplitude $A(t)$ and phase $\phi(t)$,

$$\zeta(t) = g(t) + \imath g_{\mathrm{H}}(t) = A(t)\exp\left(\imath\phi(t)\right). \tag{51}$$

The signal $g_{\mathrm{H}}(t)$ in Eq. (51) is the Hilbert transform (HT) of $g(t)$, which is defined by

$$\mathcal{H}(g(t)) \equiv g_{\mathrm{H}}(t) = \frac{1}{\pi}\mathrm{P.V.}\int_{-\infty}^{+\infty} \frac{g(\tau)}{t-\tau}\mathrm{d}\tau \tag{52}$$

and P.V. means that the integral is calculated according to the Cauchy principal value to handle the singularity at $\tau = t$ [14, 67, 69]. By Eq. (51) each time $t$ is related to an instantaneous phase value $\phi(t)$. The phase series can then be extracted from the relation

$$\tan(\phi(t)) = \frac{g_{\mathrm{H}}(t)}{g(t)}. \tag{53}$$

The Hilbert transform in Eq. (52) is equivalent to a convolution of $1/(\pi t)$ with $g(t)$ (see Eq. (14)), and according to the convolution theorem, Eq. (13), Eq. (52) can be written as

$$\frac{1}{\pi t} * g(t) \longleftrightarrow -\imath\,\mathrm{sgn}(f)G(f), \tag{54}$$

since the Fourier transform of $1/(\pi t)$ is $-\imath\,\mathrm{sgn}(f)$. Thus, for physically relevant frequencies $f > 0$, $G(f)$, the Fourier transform of $g(t)$, has to be multiplied by

$$-\imath = \exp\left(-\imath\pi/2\right). \tag{55}$$

The computing algorithm to calculate the Hilbert transform would be the following: (i) perform the FFT of the original signal $g(t)$, (ii) shift the phases of $G(f)$ by $-\pi/2$ for every frequency component by swapping the imaginary and the real parts, (iii) multiply the new imaginary part by $-1$, and (iv) apply the inverse FFT on the modified function $G_{\mathrm{mod}}(f)$.

A drawback of the Hilbert transform is that it assumes signals to be (quasi-) sinusoidal. To calculate, for instance, the instantaneous phase of force profiles in human gait, the wavelet transform is preferable. Following Eq. (26), the wavelet coefficients at a particular scale $a$ can be calculated by

$$W_a(t) = g(t) * \psi^*(t), \tag{56}$$

where $\psi^*(t)$ is a complex wavelet which has to be chosen according to the typical form of the signal. Similar as in the analytic signal approach (Eq. (51)), the instantaneous phase $\phi_W(t)$ of $g(t)$ can be calculated from [45]

$$W_a(t) = A_W(t)\exp\left(\imath\phi_W(t)\right) \tag{57}$$

($A_W(t)$ is the instantaneous amplitude of $g(t)$).

### 5.2.3 Phase Synchronization Analysis (PSA)

After the phases of two signals were calculated, several measures exist to quantify phase synchronization between both signals. We will focus on three of the most important measures, suggested for example in [67].

**a) Synchronization index based on Shannon entropy**

For this measure the cyclic relative phase has to be calculated by help of Eq. (47). The distribution of the differences series $\Psi_{n,m}(t)$ in a histogram of $M$ bins (with bin width $2\pi/M$) is then evaluated. Taking $p_l$ as the probability of the $l$-th bin of the histogram being occupied, the Shannon entropy is defined as

$$S = -\sum_{l=1}^{M}(p_l \ln p_l). \tag{58}$$

Obviously, if we find a uniform distribution of $\Psi_{n,m}(t)$, meaning $p_l = 1/M$, the Shannon entropy will be maximal and one gets

$$S = -M\frac{1}{M}\ln\frac{1}{M} = \ln M =: S_{\max}. \tag{59}$$

In this case there is no phase synchronization between the two signals. On the other hand, a perfect phase synchronization would lead to a single peak (with $p = 1$) in the histogram and $S = 0$. Hence, a suitable index to quantify phase synchronization is

$$\rho_{n,m} = \frac{S_{\max} - S}{S_{\max}}, \tag{60}$$

which results in $\rho_{n,m} \approx 0$ in case of independence between both signals, and $\rho_{n,m} \approx 1$ for a narrow distribution of $\Psi_{n,m}(t)$ (small entropy) corresponding to strong phase synchronization.

A drawback of this method is that $\rho_{n,m}$ is not parameter free but depends on the number of bins in the histogram. One way of defining the optimal number of bins is suggested in [54].

**b) Synchronization index based on the distribution on the unit circle**

The cyclic relative phase, $\Psi_{n,m}(t)$, can be seen as an angle describing the position of a point on the unit circle in the complex plane. The abscissa (real part) is given by $\cos\Psi_{n,m}(t)$, the ordinate (imaginary part) by $\sin\Psi_{n,m}(t)$. If $\Psi_{n,m}(t)$ is uniformly distributed on the unit circle, the mean of real and imaginary part will be zero in each case. On the other hand, if $\Psi_{n,m}(t)$ accumulates around one value, the "center of mass" [69] will be shifted from the origin. Hence, the index

$$\gamma^2_{n,m} = \langle\cos\Psi_{n,m}(t)\rangle^2 + \langle\sin\Psi_{n,m}(t)\rangle^2 \tag{61}$$

is defined to measure phase synchronization and $\gamma = 0$ corresponds to no phase synchronization whereas $\gamma \approx 1$, if $\Psi_{n,m}(t)$ is centered around one value. The advantage of $\gamma$ is that it is parameter free, i.e., no parameter, as for example the number of bins in the histogram, has to be chosen. A drawback of this measure could be if $\Psi_{n,m}(t)$ accumulates around two values at opposite angles, for example 0 and $\pi$. In this case the center of mass will be not very different from the origin although strong phase synchronization may be present. In order to reliably detect phase synchronization, it is helpful to calculate both indices, $\rho_{n,m}$ and $\gamma_{n,m}$.

**c) Synchrogram**

In the synchrogram, which is a stroboscopic technique, we observe the phase of the slower oscillator, $\phi^s \bmod 2\pi$, at the instants of time, $t_i$, when the phase of the faster oscillator, $\phi^f \bmod 2\pi$, attains a certain fixed value $\theta$, $\phi^s(t_i) \bmod 2\pi = \theta$. Plotting

$$\psi(t_i) = \phi^s(t_i) \bmod 2\pi \tag{62}$$

versus $t_i$ would exhibit $n$ horizontal lines (or bands) in case of $n$:1 synchronization, meaning that all phase values $\phi^f(t_j) \bmod 2\pi = \theta$ (with $j = i + kn$, where $k \in \mathbb{N}$ and $i$ is fixed) are found at the same phase $\phi^s$. In general, to detect $n : m$ synchronization, the phase of the slower oscillator is wrapped to the interval $[0, 2m\pi]$ and Eq. (62) is re-written

$$\psi_m(t_i) = \phi^s(t_i) \bmod 2m\pi. \tag{63}$$

The advantage of the synchrogram is that, in contrast to the cyclic relative phase (Eq. (47)) only one integer, $m$, has to be chosen by trial.

A prominent application of the synchrogram method is studying phase synchronization in the cardio-respiratory system [71, 72]. However, so far synchrograms could only be evaluated by visual inspection, which is not suitable to analyze synchronization between long signals. In order to detect cardio-respiratory synchronization automatically in long data, we developed a new method [6] which is based on the following steps (see also Fig. 1):

1. Starting with a synchrogram determined by Eq. (63) [Fig. 1(a)], for each synchronization ratio $n : m$ we replace the $n$ phase points in $\psi_m(t_i)$ in each $m$ respiratory cycles by the averages $\langle \psi_m(t_i) \rangle$ calculated over the corresponding phase points in time windows from $t_i - \tau/2$ to $t_i + \tau/2$ [Fig. 1(b)].
2. The algorithm deletes all phase points $\langle \psi_m(t_i) \rangle$ where the mean standard deviation of the $n$ points in each $m$ breathing cycles, $\langle \sigma \rangle_n$, is larger than $2m\pi/n\lambda$.
3. Only those phase points $\langle \psi_m(t_i) \rangle$ in not interrupted episodes are kept, which exceed a minimal duration of $T$ seconds [Fig. 1(c)].

The parameters $\tau = T = 30$ s and $\lambda = 5$ were found by optimization and surrogate data analysis, where heartbeat and breathing signals from different subjects were randomly combined [6].

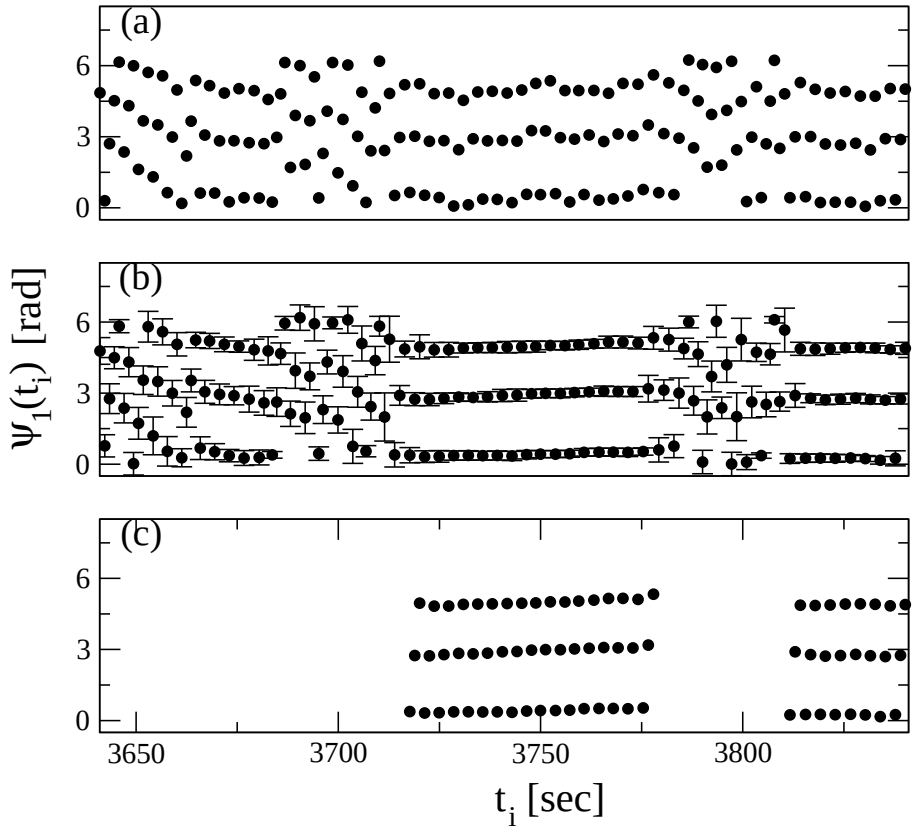


Figure 1: Illustration of our automated phase synchronization detector: (a) section of a typical synchrogram in raw form, (b) same section as in (a) after applying a moving average filter with windows $\tau = 30$ s around each breathing cycle; the window averages are shown together with their standard deviations (error bars), (c) contiguous phase points of (b) where the standard deviation is below a certain threshold (see text) are detected as synchronization episodes if their duration exceed $T = 30$ s.

### 5.2.4 Modified Cross-Correlation Analysis

The cross-correlation function between two time series $\mathcal{X}$ and $\mathcal{Z}$ is defined by (cf. Eqs. (2) and (15))

$$C_\times(s) = \frac{1}{N-s} \sum_{i=1}^{N-s} \frac{(x_i - \langle x \rangle)(z_{i+s} - \langle z \rangle)}{\sigma_x \sigma_z}, \tag{64}$$

where $\langle x \rangle, \langle z \rangle$ are the means and $\sigma_x, \sigma_z$ are the standard deviations of $\mathcal{X}$ and $\mathcal{Z}$, respectively. In order to study the strength of interrelations between different signals one could simply compare the maximum values of $C_\times(s)$ between their pairs. However, as shown in [62], the maximum value of the cross-correlation function strongly depends on the autocorrelations in the signals $\mathcal{X}$ and $\mathcal{Z}$. In particular, if the autocorrelations are stronger, the cross-correlation

is also stronger. Hence, to avoid the spurious detection of interrelations in signals of different origin, we developed a new kind of cross-correlation analysis which is based on four steps:

1. We first divide the signals into $M$ overlapping segments of equal length $L$.

2. The cross-correlation function $C_\times(s)$, Eq. (64), is calculated in each segment and a cross-correlation time delay is defined by the value of $s$ where $C_\times(s)$ is maximal:

$$\delta = \max_s |C_\times(s)| \,. \tag{65}$$

   (To account for the directionality in coupling we further distinguish between positive and negative time delays and treat them differently.)

3. In order to distinguish between real and randomly occurring peaks in $C_\times(s)$, we only take into account segments where $\delta$ was stable, i.e. did not change in $k$ out of $l$ consecutive segments by more than $\pm\Delta$, and defined the signals as linked.

4. A new binary time series was created describing the interrelation between both signals in each segment, either as linked ("1"), or not linked ("0"). Subsequent averaging of these time series determines the probability two signals were linked independent of their autocorrelations.

The parameters $k$, $l$ and $\Delta$ have to be found again by optimization and surrogate data analysis. In our study [11] we set $k = 5$, $l = 10$ and $\Delta = 1$ s.
This modified cross-correlation analysis provides the basis for investigating physiological networks constructed from data of very different origin by systematically excluding their autocorrelation properties.

# References


[1] Heart rate variability – standards of measurement, physiological interpretation and clinical use. *Circulation*, 93:1043–65, 1996. Task Force of The European Society of Cardiology and The North American Society of Pacing and Electrophysiology.

[2] P.S. Addison. *The Illustrated Wavelet Transform Handbook*. Institute of Physics, Bristol, 2002.

[3] L.A.N. Amaral, A.L. Goldberger, P.Ch. Ivanov, and H.E. Stanley. Scale-independent measures and pathologic cardiac dynamics. *Physical Review Letters*, 81:2388–2391, 1998.

[4] Y. Ashkenazy, P.Ch. Ivanov, S. Havlin, C.-K. Peng, A.L. Goldberger, and H.E. Stanley. Magnitude and sign correlations in heartbeat fluctuations. *Physical Review Letters*, 86:1900–1903, 2001.

[5] R. Bartsch, T. Hennig, A. Heinen, S. Heinrichs, and P. Maass. Statistical analysis of fluctuations in the ECG morphology. *Physica A*, 354:415–431, 2005.

[6] R. Bartsch, J. Kantelhardt, T. Penzel, and S. Havlin. Experimental evidence for phase synchronization transitions in the human cardio-respiratory system. *Physical Review Letters*, 98:054102(4), 2007.

[7] R. Bartsch, J. Kantelhardt, A.Y. Schumann, T. Penzel, S. Havlin, and P.Ch. Ivanov. Cardiorespiratory coupling during sleep in healthy humans. Preprint to be submitted to *Proceedings of the National Academy of Sciences of the United States of America*.

[8] R. Bartsch, M. Plotnik, J.W. Kantelhardt, S. Havlin, N. Giladi, and J.M. Hausdorff. Fluctuation and synchronization of gait intervals and gait force profiles distinguish stages of parkinson's disease. *Physica A*, 383:455–465, 2007.

[9] R. Bartsch, M. Plotnik, M. Leshem, S. Havlin, and J.M. Hausdorff. Studying bilateral coordination of human gait in young subjects and patients with parkinson's disease. To be submitted to *Experimental Brain Research*.

[10] A. Bashan, R. Bartsch, J.W. Kantelhardt, and S. Havlin. Comparison of detrending methods for fluctuation analysis. Accepted for publication in *Physica A*, 2008.

[11] A. Bashan, R. Bartsch, J.W. Kantelhardt, T. Penzel, A.Y. Schumann, P. Lavie, and S. Havlin. Dynamic analysis of physiological networks during sleep. Preprint to be submitted to *Europhysics Letters*.

[12] J.B. Bassingthwaighte, L.S. Liebovitch, and B.J. West. *Fractal Physiology*. Oxford University Press, New York, 1994.

[13] Ch. Blatter. *Wavelets - Eine Einführung*. Vieweg Verlag, Braunschweig/Wiesbaden, 1998.

[14] I.N. Bronstein, K.A. Semendjajew, G. Musiol, and H. Mühlig. *Taschenbuch der Mathematik für Ingenieure und Studenten*. Verlag Harri Deutsch, Frankfurt am Main, 1995.

[15] A. Bunde and S. Havlin, editors. *Fractals and Disordered Systems*. Springer-Verlag, Berlin, 1996.

[16] A. Bunde, S. Havlin, J.W. Kantelhardt, T. Penzel, J.H. Peter, and K. Voigt. Correlated and uncorrelated regions in heart-rate fluctuations during sleep. *Physical Review Letters*, 85:3736–3739, 2000.

[17] A. Bunde and J.W. Kantelhardt. Langzeitkorrelationen in der Natur: von Klima, Erbgut und Herzrhythmus. *Physikalische Blätter*, 57:49–54, 2001.

[18] W.B. Cannon. Organization for physiological homeostasis. *Physiological Reviews*, 9:399–431, 1929.

[19] I. Daubechies. *Ten Lectures on Wavelets*. S.I.A.M., Philadelphia, 1992.

[20] J.F. Eichner. *Über die Statistik der Maximawerte und Wiederkehrintervalle in langzeitkorrelierten Systemen*. Dissertation thesis in Physics, Justus-Liebig-Universität Gießen, Germany, 2005.

[21] J. Feder. *Fractals*. Plenum Press, New York, 1988.

[22] D. Gabor. Theory of communication. *Journal of the Institution of Electrical Engineering*, 93:429–457, 1946.

[23] L. Glass and M.C. Mackey. *From Clocks to Chaos: The Rhythms of Life*. Princeton University Press, Princeton, 1988.

[24] J.M. Gottman. *Time-series analysis – A comprehensive introduction for social scientists*. Cambridge University Press, Cambridge, 1981.

[25] C. Hamann, R. Bartsch, A.Y. Schumann, T. Penzel, S. Havlin, and J.W. Kantelhardt. To be submitted to *Physical Review E*.

[26] J.M. Hausdorff, Y. Balash, and N. Giladi. Time series analysis of leg movements during freezing of gait in parkinson's disease: akinesia, rhyme or reason? *Physica A*, 321:565–570, 2003.

[27] J.M. Hausdorff, S.L. Mitchell, R. Firtion, C.-K. Peng, M.E. Cudkowicz, J.Y. Wei, and A.L. Goldberger. Altered fractal dynamics of gait: reduced stride-interval correlations with aging and huntington's disease. *Journal of Applied Physiology*, 82:262–269, 1997.

[28] S. Havlin, R. Blumberg Selinger, M. Schwartz, H.E. Stanley, and A. Bunde. Random multiplicative processes and transport structures with correlated spatial disorder. *Physical Review Letters*, 61:1438–1441, 1988.

[29] H.V. Huikuri, T.H. Makikallio, C.-K. Peng, A.L. Goldberger, U. Hintze, and M. Moller. Fractal correlation properties of R-R interval dynamics and mortality in patients with depressed left ventricular function after an acute myocardial infarction. *Circulation*, 101:47–53, 2000.

[30] H.E. Hurst. Long-term storage capacity of reservoirs. *Transactions of the American Society of Civil Engineers*, 116:770–808, 1951.

[31] H.E. Hurst. Methods of using long-term storage in reservoirs. *Proceedings of the Institution of Civil Engineers*, pages 519–577, 1956. Part I.

[32] H.E. Hurst, R.P. Black, and Y.M. Simaika. *Long-term storage, an experimental study*. Constable & Co. Ltd., London, 1965.

[33] B.W. Hyndman. The role of rhythms in homeostasis. *Kybernetik*, 15:227–236, 1974.

[34] P.Ch. Ivanov, L.A.N. Amaral, A.L. Goldberger, S. Havlin, M.G. Rosenblum, H.E. Stanley, and Z.R. Struzik. From $1/f$ noise to multifractal cascades in heartbeat dynamics. *Chaos*, 11:641–652, 2001.

[35] P.Ch. Ivanov, L.A.N. Amaral, A.L. Goldberger, S. Havlin, M.G. Rosenblum, Z.R. Struzik, and H.E. Stanley. Multifractality in human heartbeat dynamics. *Nature*, 399:461–465, 1999.

[36] P.Ch. Ivanov, L.A.N. Amaral, A.L. Goldberger, and H.E. Stanley. Stochastic feedback and the regulation of biological rhythms. *Europhysics Letters*, 43:363–368, 1998.

[37] P.Ch. Ivanov, A. Bunde, L.A.N. Amaral, S. Havlin, J. Fritsch-Yelle, R.M. Baevsky, H.E. Stanley, and A.L. Goldberger. Sleep-wake differences in scaling behavior of the human heartbeat: analysis of terrestrial and long-term space flight data. *Europhysics Letters*, 48:594–600, 1999.

[38] P.Ch. Ivanov, M.G. Rosenblum, C.-K. Peng, J. Mietus, S. Havlin, H.E. Stanley, and Goldberger A.L. Scaling behaviour of heartbeat intervals obtained by wavelet-based time-series analysis. *Nature*, 383:323–327, 1996.

[39] J.W. Kantelhardt, Y. Ashkenazy, P.Ch. Ivanov, A. Bunde, S. Havlin, T. Penzel, J.-H. Peter, and H.E. Stanley. Characterization of sleep stages by correlations in the magnitude and sign of heartbeat increments. *Physical Review E*, 65:051908(6), 2002.

[40] J.W. Kantelhardt, E. Koscielny-Bunde, H.H.A. Rego, S. Havlin, and A. Bunde. Detecting long-range correlations with detrended fluctuation analysis. *Physica A*, 295:441–454, 2001.

[41] J.W. Kantelhardt, E. Koscielny-Bunde, D. Rybski, P. Braun, A. Bunde, and S. Havlin. Long-term persistence and multifractality of precipitation and river runoff records. *Journal of Geophysical Research – Atmospheres*, 111:D01106, 2006.

[42] J.W. Kantelhardt, S.A. Zschiegner, E. Koscielny-Bunde, S. Havlin, A. Bunde, and H.E. Stanley. Multifractal detrended fluctuation analysis of nonstationary time series. *Physica A*, 316:87–114, 2002.

[43] R. Karasik, N. Sapir, Y. Ashkenazy, P.Ch. Ivanov, I. Dvir, P. Lavie, and S. Havlin. Correlation differences during rest and exercise. *Physical Review E*, 66:062902(4), 2002.

[44] M. Kobayashi and T. Musha. $1/f$ fluctuation of heartbeat period. *IEEE Transactions on Biomedical Engineering*, 29:456–457, 1982.

[45] J. Lachaux, E. Rodriguez, J. Martinerie, and F. Varela. Measuring phase-synchrony in brain signals. *Human Brain Mapping*, 8:194–208, 1999.

[46] P. Lavie. *The Enchanted World of Sleep*. Yale University Press, New Haven, 1996.

[47] H.A. Makse, S. Havlin, M. Schwartz, and H.E. Stanley. Method for generating long-range correlations for large systems. *Physical Review E*, 53:5445–5449, 1996.

[48] S. Mallat and W.L. Hwang. Singularity detection and processing with wavelets. *IEEE Transactions on Information Theory*, 38:617–643, 1992.

[49] E.W. Montroll and M.F. Shlesinger. *Nonequilibrium phenomena II: from stochastics to hydrodynamics*, volume 11 of *Studies in Statistical Mechanics*, chapter 1. On the wonderful world of random walks, pages 1–121. North-Holland Physics Publishing, Amsterdam, 1984.

[50] C.J. Morales and E.D. Kolaczyk. Wavelet-based multifractal analysis of human balance. *Annals of Biomedical Engineering*, 30:588–597, 2002.

[51] R. Mrowka, A. Patzak, and M.G. Rosenblum. Quantitative analysis of cardiorespiratory synchronization in infants. *International Journal of Bifurcation and Chaos*, 10:2479–2488, 2000.

[52] T. Müller, M. Lauk, M. Reinhard, A. Hetzel, C.H. Lücking, and J. Timmer. Estimation of delay times in biological systems. *Annals of Biomedical Engineering*, 31:1423–1439, 2003.

[53] J.F. Muzy, E. Bacry, and A. Arneodo. Wavelets and multifractal formalism for singular signals: Application to turbulence data. *Physical Review Letters*, 67:3515–3518, 1991.

[54] R. Otnes and L. Enochson. *Digital Time Series Analysis*. John Wiley & Sons, New York, 1972.

[55] C.-K. Peng, S.V. Buldyrev, J.F. Hausdorff, S. Havlin, J.E. Mietus, M. Simons, H.E. Stanley, and A.L. Goldberger. Non-equilibrium dynamics as an indispensable characteristic of a healthy biological system. *Integrative Psychological and Behavioral Science*, 29:283–293, 1994.

[56] C.-K. Peng, S.V. Buldyrev, S. Havlin, M. Simons, H.E. Stanley, and A.L. Goldberger. Mosaic organization of DNA nucleotides. *Physical Review E*, 49:1685–1689, 1994.

[57] C.-K. Peng, S. Havlin, H.E. Stanley, and A.L. Goldberger. Quantification of scaling exponents and crossover phenomena in nonstationary heartbeat time series. *Chaos*, 5:82–87, 1995.

[58] C.-K. Peng, J.E. Mietus, J.M. Hausdorff, S. Havlin, H.E. Stanley, and A.L. Goldberger. Long-range anti-correlations and non-gaussian behavior of the heartbeat. *Physical Review Letters*, 70:1343–1346, 1993.

[59] E.A. Phillipson. Control of breathing during sleep. *The American review of respiratory disease*, 118:909–939, 1978.

[60] E.A. Phillipson, E. Murphy, and L.F. Kozar. Regulation of respiration in sleeping dogs. *Journal of Applied Physiology*, 40:688–693, 1976.

[61] A. Pikovsky, J. Kurths, and M. Rosenblum. *Synchronization: A Universal Concept in Nonlinear Sciences*. Cambridge University Press, Cambridge, 2001.

[62] B. Podobnik, D.F. Fu, H.E. Stanley, and P.Ch. Ivanov. Power-law autocorrelated stochastic processes with long-range cross-correlations. *The European Physical Journal B*, 56:47–52, 2007.

[63] W.H. Press, B.P Flannery, S.A. Teukolsky, and W.T. Vetterling. *Numerical Recipes in C*. Cambridge University Press, Cambridge, 1992.

[64] R. Quian Quiroga, A. Kraskov, T. Kreuz, and P. Grassberger. Performance of different synchronization measures in real data: A case study on electroencephalographic signals. *Physical Review E*, 65:041903(14), 2002.

[65] M.G. Rosenblum, L. Cimponeriu, A. Bezerianos, A. Patzak, and R. Mrowka. Identification of coupling direction: Application to cardiorespiratory interaction. *Physical Review E*, 65:041909(11), 2002.

[66] M.G. Rosenblum, A.S. Pikovsky, and J. Kurths. Phase synchronization of chaotic oscillators. *Physical Review Letters*, 76:1804–1807, 1996.

[67] M.G. Rosenblum, A.S. Pikovsky, C. Schäfer, P.A. Tass, and J. Kurths. *Neuro-Informatics and Neural Modelling (Handbook of Biological Physics)*, volume 4, chapter 9. Phase synchronization: from theory to data analysis, pages 279–321. Elsevier Science B.V., Amsterdam, 2001.

[68] S. Rostig, J.W. Kantelhardt, T. Penzel, W. Cassel, J.H. Peter, C. Vogelmeier, H.F. Becker, and A. Jerrentrup. Nonrandom variability of respiration during sleep in healthy humans. *Sleep*, 28:411–417, 2005.

[69] D. Rybski. *Untersuchungen von Korrelationen, Trends und synchronem Verhalten in Klimazeitreihen.* Dissertation thesis in Physics, Justus-Liebig-Universität Gießen, Germany, 2006.

[70] D. Rybski, S. Havlin, and A. Bunde. Phase synchronization in temperature and precipitation records. *Physica A*, 320:601–610, 2003.

[71] C. Schäfer, M.G. Rosenblum, H.H. Abel, and J. Kurths. Synchronization in the human cardiorespiratory system. *Physical Review E*, 60:857–870, 1999.

[72] C. Schäfer, M.G. Rosenblum, J. Kurths, and H.H. Abel. Heartbeat synchronized with ventilation. *Nature*, 392:239–240, 1998.

[73] T. Schreiber and A. Schmitz. Improved surrogate data for nonlinearity tests. *Physical Review Letters*, 77:635–638, 1996.

[74] T. Schreiber and A. Schmitz. Surrogate time series. *Physica D*, 142:346–382, 2000.

[75] Y. Shimizu, S. Thurner, and K. Ehrenberger. Multifractal spectra as a measure of complexity in human posture. *Fractals*, 10:103–116, 2002.

[76] H.E. Stanley. *Introduction to Phase Transitions and Critical Phenomena.* Oxford University Press, London, 1971.

[77] H.E. Stanley. Power laws and universality. *Nature*, 378:554(1), 1995.

[78] M.S. Taqqu, V. Teverovsky, and W. Willinger. Estimators for long-range dependence: An empirical study. *Fractals*, 3:785–798, 1995.

[79] P. Tass, M.G. Rosenblum, J. Weule, J. Kurths, A. Pikovsky, J. Volkmann, A. Schnitzler, and H.J. Freund. Detection of $n:m$ phase locking from noisy data: Application to magnetoencephalography. *Physical Review Letters*, 81:3291–3294, 1998.

[80] S. Thurner, M.C. Feurstein, and M.C. Teich. Multiresolution wavelet analysis of heartbeat intervals discriminates healthy patients from those with cardiac pathology. *Physical Review Letters*, 80:1544–1547, 1998.

[81] E. Toledo, S. Akselrod, I. Pinhas, and D. Aravot. Does synchronization reflect a true interaction in the cardiorespiratory system? *Medical Engineering & Physics*, 24:45–52, 2002.

[82] B. van der Pol and J. van der Mark. The heartbeat considered as a relaxation oscillation, and an electrical model of the heart. *The London, Edinburgh and Dublin Philosophical Magazine and Journal of Science*, 6:763–775, 1928.